Clin Orthop Relat Res (2011) 469:2953–2970
DOI 10.1007/s11999-011-1916-9

SOCIETY AWARDS

The 2011 ABJS Nicolas Andry Award: 'Lab'-in-a-Knee

In Vivo Knee Forces, Kinematics, and Contact Analysis

Darryl D. D'Lima MD, PhD, Shantanu Patil MD, Nicolai Steklov BS, Clifford W. Colwell Jr MD

Received: 1 November 2010 / Accepted: 2 May 2011 / Published online: 20 May 2011

Abstract

Background Tibiofemoral forces are important in the design and clinical outcomes of TKA. We developed a tibial tray with force transducers and a telemetry system to directly measure tibiofemoral compressive forces in vivo. Knee forces and kinematics traditionally have been measured under laboratory conditions. Although this approach is useful for quantitative measurements and experimental studies, the extrapolation of results to clinical conditions may not always be valid.

Questions/purposes We therefore developed wearable monitoring equipment and computer algorithms for classifying and identifying unsupervised activities outside the laboratory.

Methods Tibial forces were measured for activities of daily living, athletic and recreational activities, and with orthotics and braces, during 4 years postoperatively. Additional measurements included video motion analysis, EMG, fluoroscopic kinematic analysis, and ground reaction force measurement. In vivo measurements were used to evaluate computer models of the knee. Finite element models were used for contact analysis and for computing knee kinematics from measured knee forces. A third-generation system was developed for continuous monitoring of knee forces and kinematics outside the laboratory using a wearable data acquisition hardware.

Results By using measured knee forces and knee flexion angle, we were able to compute femorotibial AP translation (−12 to +4 mm), mediolateral translation (−1 to 1.5 mm), axial rotation (−3° to 12°), and adduction-abduction (−1° to +1°). The neural-network-based classification system was able to identify walking, stair-climbing, sit-to-stand, and stand-to-sit activities with 100% accuracy.

Conclusions Our data may be used to improve existing in vitro models and wear simulators, and enhance prosthetic designs and biomaterials.

Introduction

Tibiofemoral forces are important in the design and clinical outcomes of TKA. These forces determine wear and cold flow in polyethylene, stress distribution in the implant, the implant-bone interface, and stress transfer to the underlying bone. Direct measurement of joint forces in vivo has been challenging because of issues with miniaturization of electronics, remote powering, long-term durability of electronic components, and safety of the implant design. Hip forces measured through telemetry typically have been lower by 160% to 400% than those predicted mathematically [4, 5]. The knee is difficult to model accurately because of its complex geometry, six degrees of freedom, and the major role soft tissues play in stabilizing and directing knee function. Modeling is complicated by the high degree of mechanical redundancy attributable to the

One of the authors (DDD) received research support from Stryker, Zimmer, Smith & Nephew, and Tornier. One of the authors (CWC) is a consultant for Stryker.
One or more of the authors (DDD, CWC) received funding from the National Institutes of Health under the following grants: R01 EB009351 and R21 AR057561.
Each author certifies that his institution has approved the human protocol for this investigation, that all investigations were conducted in conformity with ethical principles of research, and that informed consent for the study was obtained.

D. D. D'Lima (✉), S. Patil, N. Steklov, C. W. Colwell Jr
Shiley Center for Orthopaedic Research and Education at Scripps Clinic, 11025 North Torrey Pines Road, Suite 200, La Jolla, CA 92037, USA
e-mail: ddlima@scripps.edu

numerous muscles involved in knee motion, some of which are biarticular. As a result, theoretic estimates of tibiofemoral forces have been inconsistent and vary widely based on the mathematical model used and the activity analyzed [6, 31, 33, 47, 58]. For example, a two-dimensional static analysis of maximum voluntary isokinetic knee extension with a single quadriceps muscle estimated peak tibiofemoral compressive forces up to 9 times body weight (×BW) [43], whereas a two-dimensional inverse dynamics model using a linear optimization algorithm to solve for the distribution of synergistic muscle forces estimated peak compressive forces of only 4 × BW during maximal voluntary effort [23]. Knee forces predicted for walking range from 1.7 × BW to 7 × BW [6, 27, 28, 47].

We developed a knee arthroplasty tibial tray with force transducers and a telemetry system to directly measure tibiofemoral compressive forces in vivo. The first tibial tray and transducer design was reported in 1996 for in vitro testing [24]. A working prototype of the telemetry and remote powering initially was presented in 1999 [15]. Subsequent years were spent in refining manufacturing techniques, improving durability, and safety testing. The instrumented prosthesis also was used intraoperatively as a trial for dynamic ligament balancing [10]. The first electronic knee prosthesis was implanted on February 27, 2004. Forces were monitored during recovery and rehabilitation in the early postoperative period and for activities of daily living and exercise during the first 24 months after surgery [11, 12]. These measurements were supplemented by video motion analysis, EMG, fluoroscopic kinematic analysis, and ground reaction force measurement.

In this paper, we summarize the design, development, and in vivo use of two generations of the electronic knee prosthesis with activities of daily living, rehabilitation, exercise, and athletic activities from several studies (Table 1). We then developed a third generation of wearable monitoring equipment and a method of computing knee kinematics using the measured in vivo force and an algorithm for classifying unsupervised activities. This enhanced capability now permits remote monitoring of patients' activities and simultaneous measurement of knee forces and kinematics, classifies the activity, and records a cyclic count of each activity.

Implant Design

Three generations of a tibial prosthesis design instrumented with force sensors and a telemetry system were developed during the course of this project (14 years). The first-generation device, implanted in one patient, contained four load cells, one in each quadrant of the tibial tray. By measuring the force on each load cell, the total axial load, the location of the center of pressure, and the distribution of forces between the medial and lateral compartments were determined. The second-generation device (Fig. 1), implanted in three patients, used 12 strain gauges that measured strain in the stem of the tibial tray, which were calibrated to yield the three forces and three moments acting on the tray. Details of the device specifications, accuracy, and preclinical testing have been reported [15, 26]. The third-generation design involved miniaturization of the external power and data acquisition equipment to a wearable belt pack (~2 pounds), enabling continuous monitoring of knee forces and kinematics outside the laboratory.

Intraoperative Use

Complications after TKA such as malalignment, instability, subluxation, excessive wear, and loosening have been attributed to poor soft-tissue balance [32, 48, 59]. Refinements in surgical technique and instrumentation and surgical navigation systems have improved component alignment [7, 19, 50, 51, 54]. Soft-tissue balance remains an art, largely driven by the surgeon's experience. Current standards involve either a distraction device that measures joint space or trial components and subjective varus-valgus stress testing. Both approaches use static assessments in full extension and at 90° flexion. Tightness or mediolateral balance at angles between 0° and 90° cannot be assessed, nor is imbalance in the AP direction addressed.

The instrumented tibial component was inserted in six cadaver knees and two patients, along with a trial femoral component and a tibial insert (Table 2) [10]. Dynamic knee forces and kinematics were recorded during passive flexion. Next, soft-tissue balance, fine tuning of the bone cuts, and selection of optimal insert thickness were performed with the help of routine tibiofemoral balancing instrumentation and trial components until the surgeon was satisfied with the ligament tension. Forces were recorded after satisfactory balance with an insert of optimal thickness and again using an insert that was 2 mm thicker than optimal.

In all knees (in vitro and in vivo), substantial measurable imbalance initially was recorded [10]. Mean imbalance after soft-tissue balancing was lower ($p < 0.01$). Residual imbalance remained at flexion angles other than 0° and 90°. Increasing the thickness of the insert by 2 mm increased tibial forces ($p < 0.01$) and exaggerated the residual imbalance during passive flexion. In all knees, balance was

Table 1. Summary of studies of the instrumented knee implant

Study number	Study name	Status	Brief summary	Publication
1	Development of an implantable electronic tibial tray	Complete	Force transducers, a telemetry system, and remote powering were developed	[15, 40]
2	Dynamic ligament balancing	Complete	The instrumented tibial tray was used as a tool for dynamic ligament balancing	[10]
3	In vivo implantation	Complete	Intraoperative and immediate postoperative tibial forces were measured	[11, 12]
4	Tibial forces during activities of daily living and rehabilitation	Complete	Tibial forces were recorded during walking, stair climbing, chair rise, stationary cycling, and exercise	[11]
5	In vivo medial and lateral tibial load distribution	Complete	A dynamic computer model was used to calculate mediolateral load and contact stress distribution	[61]
6	Correlation between the knee adduction torque and medial contact force	Complete	In vivo medial tibial force correlated with external adduction moment	[62]
7	Polyethylene contact stresses determined with in vivo tibial force measurement and fluoroscopic analysis	Complete	A finite element model was developed to compute in vivo tibiofemoral contact stresses for various activities	[13]
8	Activity-dependent tibial loading characteristics	Complete	Forces and motion sustained by the knee are unique and activity-dependent	[13]
9	Development of the second-generation multiaxial force-sensing tibial prosthesis	Complete	A second-generation prosthesis capable of measuring all six components of forces was validated	[26]
10	In vivo knee moments and shear after TKA	Complete	Tibial shear forces and moments were measured in vivo during activities of daily living	[9]
11	Analysis of knee forces while rising from a chair	In progress	The effect of seat height on the forces and moments during chair rise was studied	[44]
12	Knee forces during recreational activities	Complete	Forces were recorded during biking, jogging, tennis, golfing, and gym exercise	[14]
13	A computational model of open kinetic chain knee extension	In progress	A computer model of dynamic knee extension was validated with in vitro and in vivo measured tibial kinematics and knee forces	[25]
14	Effect of bearing congruency, thickness, and alignment on stresses in unicompartmental knee arthroplasties	Complete	In vivo knee forces were used to compute polyethylene stresses in a model assessing four unicompartmental knee designs	[49]
15	Dual-plane fluoroscopy and knee forces	Complete	In vivo contact kinematics and contact forces of the knee during dynamic weightbearing activities were analyzed	[55]
16	Sensitivity of knee arthroplasty contact calculations to kinematic measurement errors	Complete	Knee arthroplasty contact calculations are highly sensitive to kinematic measurement errors	[17]
17	Effective gait patterns for offloading the medial compartment of the knee	Complete	Gait modification strategies reduced medial compartmental forces	[18]
18	Development of a wearable telemetry data acquisition system	In progress	The data acquisition system was miniaturized to a belt pack for continuous monitoring of patient activity and knee forces	Current study
19	Automated classification of daily activities based on in vivo knee forces and kinematics	In progress	A pattern recognition algorithm was developed to classify activities based on measured knee forces and kinematics	Current study

Table 1. continued

Study number	Study name	Status	Brief summary	Publication
20	Prediction of knee kinematics from measured in vivo knee forces	In progress	A novel technique was used to compute knee kinematics directly from measured knee forces	Current study
21	Knee forces during downhill skiing after TKA	In progress	Knee forces during downhill skiing were measured to develop more scientific rationale for post-TKA activities	Current study
22	Decreased knee adduction moment does not guarantee decreased medial contact force during gait	Complete	In vivo gait data were used to assess whether knee adduction moment decreases accurately to predict decreases in medial contact force	[56]
23	Changes in in vivo knee loading with a variable-stiffness intervention shoe correlate with changes in the knee adduction	Complete	Changes in medial joint loading were assessed in patient walking with a variable-stiffness intervention shoe	[16]

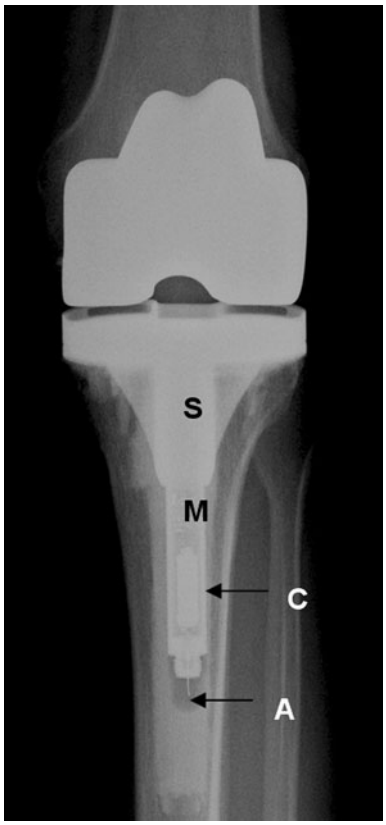

Fig. 1 A postoperative radiograph shows the instrumented second-generation tibial prosthesis. S = hollow strain-gauge portion of the stem; M = location of microprocessor; C = internal coil; A = transmitting antenna. (Published with permission from Elsevier from D'Lima DD, Patil S, Steklov N, Chien S, Colwell CW Jr. In vivo knee moments and shear after total knee arthroplasty. *J Biomech.* 2007; 40(suppl 1):S11–S17.)

achieved in extension and 90° flexion based on our definition of acceptable balance. Nevertheless, dynamic measurements revealed substantial discrepancies at other angles, which explains some of the variations in knee function and knee kinematics reported after TKA and the reported incidences of midflexion knee instability. The standard balancing instrumentation could not detect or correct imbalance in the AP direction.

Table 2. Demographic data for the four subjects

Subject	Gender	Age (years)	Weight (kg)	Height (m)
1	Male	80	67	1.64
2	Male	83	74	1.80
3	Male	79	80	1.73
4	Female	67	89	1.63

Insert thickness is a critical factor affecting knee tightness. Even a 2-mm increase in insert thickness resulted in a substantial increase in tibial forces, which emphasizes the need for balancing the ligaments and obtaining optimum knee stability. Insert thickness is selected subjectively based on the surgeon's "feel" for knee tightness during surgery. Precisely measuring forces during surgery may help quantify knee tightness, which then can be correlated with postoperative outcome.

Current-generation computer-aided surgical navigation systems cannot directly address soft-tissue balance and knee tightness [48, 50, 51]. An instrumented tibial prosthesis can enhance the value of such navigation tools in achieving reproducible clinical outcomes.

Early Postoperative Measurement of Knee Forces

During the first 3 postoperative weeks of the patients' recovery, tibial forces were monitored during active and passive knee flexion, active and passive straight-leg rise,

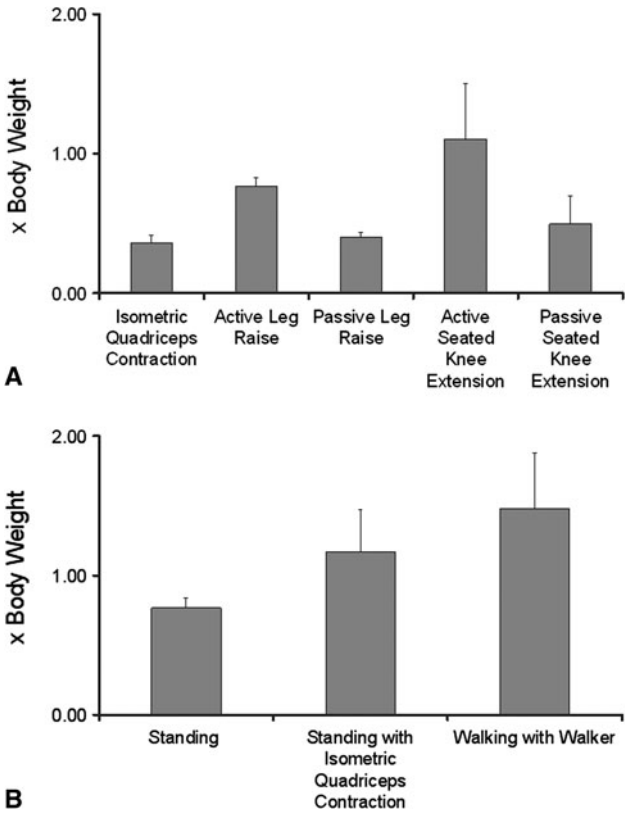

Fig. 2A–B All patients were able to bear weight on the surgically treated limb on postoperative Day 1 with the help of a walker. The mean peak axial forces (± SD) (n = ~6 trials per subject) generated during the first 3 weeks of rehabilitation for (**A**) nonweightbearing activities and (**B**) weightbearing activities are shown.

during partial weightbearing using a walker, walking, stair climbing, rising from a chair, and standing on both legs with and without support (Fig. 2) [12].

Activities of Daily Living

Peak axial knee forces were measured in all four patients (average of six trials per activity per subject), tibial shear and moments were measured in the three patients implanted with the second-generation implant. In-depth biomechanical analyses were performed for each activity relating tibial forces to knee kinematics and correlating with ground reaction forces, external flexion, and adduction moments. Only key results are summarized here.

Level Walking

Peak tibial forces during walking increased steadily during the first 12-month postoperative period and remained steady after that at a mean (± SD) 2.5 × BW (± 0.4) [11, 12]. These peak tibial forces were within the predicted range

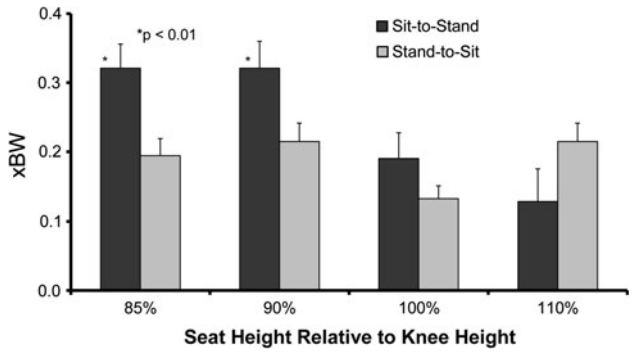

Fig. 3 Anterior tibial shear was greater ($p < 0.01$) at lower seat heights during the chair-rise activity.

(2–4 × BW [41]), slightly lower (3–3.3 × BW [53]), or substantially lower (7.1 × BW [47]) than reported mathematical models.

Stair Climbing

Stair climbing is another common activity of daily living, with the ratio of stair climbing cycles to walking cycles averaging approximately 1:25 in patients with THA [39]. Tibial forces during stair climbing increased to a mean of 3.2 × BW at 1 year [11]. This result was substantially lower than that reported for computational models [53].

Chair Rise

Pain or reduction in knee function affects the ability to rise from a chair, particularly in the older population. The height of the chair seat is a major factor affecting ability to rise from a chair [57]. Peak tibial forces were not affected by changing seat height. Peak anterior shear components were small (range, 0.1–0.3 × BW) but varied with seat height ($p = 0.002$) (Fig. 3) [44]. Flexion moments generated at the tibial tray correlated strongly ($R^2 = 0.79$) with peak flexion angle during chair rise (Fig. 4). As the flexion moment on the tibial tray is generated by net joint reaction force, an increasing flexion moment with increasing flexion angle is consistent with femoral rollback. This flexion moment on the tray may affect the bone-implant interface owing to the generation of an anterior lift-off force at the tibial tray.

Recreation and Exercise

The lengthening of life expectancy and higher overall fitness of the age group of patients undergoing TKAs continue to raise the bar on durability and survival of the

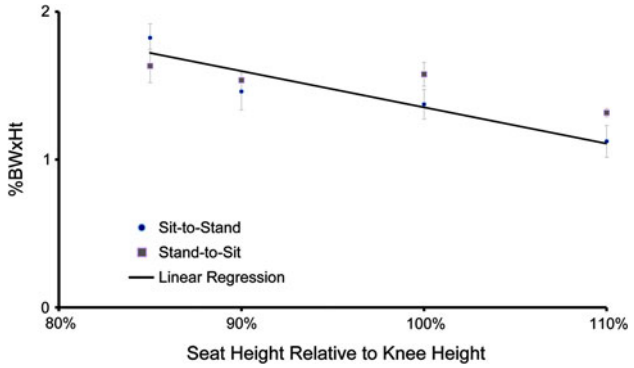

Fig. 4 An inverse linear correlation was found between the flexion moment at the tibial tray and the relative seat height. This is consistent with the occurrence of femoral rollback with increasing flexion seen with lower relative seat height. BW = body weight; Ht = height.

prosthetic components. Which activities generate forces in a physiologically desirable range and do not jeopardize durability of the arthroplasty are unknown. Conventional wisdom is that low-impact activities are safer than high-impact activities. Surgeons' recommendations are based on subjective opinions without quantitative measurements of knee forces and are not always consistent [20, 37]. The results of clinical outcomes are mixed, with some studies reporting increased component failure in more active patients and others reporting no difference [8, 22, 30, 35, 37, 38]. We directly measured tibial forces in vivo during exercise and various recreational activities at 1 year postoperatively (Fig. 5) [14].

Walking

Tibial forces were measured during treadmill walking (Star Trac TR4500; Star Trac, Irvine, CA, USA) at speeds ranging from 1 to 4 miles/hour. Peak forces remained in the range of 1.8 to 2.2 × BW for treadmill walking at the speeds tested (Fig. 5A) [14]. Knee forces during treadmill walking (2.05 ± 0.20 × BW) were lower than those measured during level walking on a laboratory floor (2.6 × BW). Treadmill speed during comfortable walking (range, 1–3 miles/hour) had no effect on peak tibial forces. A speed comparable to power walking (4 miles/hour) generated higher forces on the treadmill (2.80 ± 0.43 × BW).

Jogging

Peak forces recorded during jogging were even higher than those recorded during power walking (Fig. 5A) [14]. Differences between peak forces generated on the treadmill (at 5 miles/hour) and those generated during jogging on the laboratory floor (subject-selected speed) were minimal. Peak ground reaction forces only increased by a mean of 40% when jogging relative to walking on the laboratory floor, indicating muscle forces contributed substantially to the increased knee forces.

Stationary Bicycling

Stationary bicycling was analyzed at various levels of difficulty and speeds ranging from 60 to 90 rpm. Tibial forces peaked at 1.03 ± 0.20 × BW [14]. Increasing the speed of bicycling from 60 to 90 rpm did not affect peak tibial forces but did affect the flexion angle at which tibia force peaked (Fig. 5B). Increasing the resistance from Level 1 to Level 5 modestly increased the peak tibial forces (by an average of 14%). In general, anterior shear was low (0.21 ± 0.01 × BW)

Golf

Golfing was analyzed in the laboratory and on a driving range. High tibial forces were generated during the golf swing (Fig. 5C, D) [14]. Much higher forces were generated in the leading knee relative to the trailing knee. A golf swing with a driver generated higher forces than with a sand wedge. Forces generated during simulated swinging in the laboratory (without a ball) were similar to those generated on the driving range. Anterior tibial shear (0.34 ± 0.01 × BW) and axial tibial torque (13.0 ± 0.33 N-m) were in the moderate range.

Tennis

Tennis was analyzed in the laboratory and on the tennis courts during actual play. Mean peak forces generated during the serve and during a forehand return were greater than those generated during the backhand return (Fig. 5E) [14]. Anterior shear was moderate (0.28 ± 0.12 × BW). Forces measured during actual play on the tennis courts were on average 12% greater than those generated during simulated strokes in the laboratory.

Skiing

Forces generated during recreational skiing vary with activity and level of difficulty. Straight skiing (cruising) on gentle slopes generated the lowest forces (1.5 ± 0.22 × BW), whereas carving the slopes (4.3 ± 0.10 × BW)

generated the highest forces (Fig. 5F). Skating and stopping generated higher forces than shuffling or slowing down by "snow-plowing". These results represent the first in vivo measurements of forces directly at the tibial tray during downhill skiing and generated greater knee forces than those previously estimated by mathematical modeling of younger subjects with normal healthy knees [34]. In general, peak forces measured on the slopes also were greater than those measured during indoor exercise on an elliptical trainer [14].

Rowing, Elliptical Trainer, and StairMaster®

Rowing on a rowing machine (Indoor Rower; Concept2, Morrisville, VT, USA), generated a peak mean tibial force

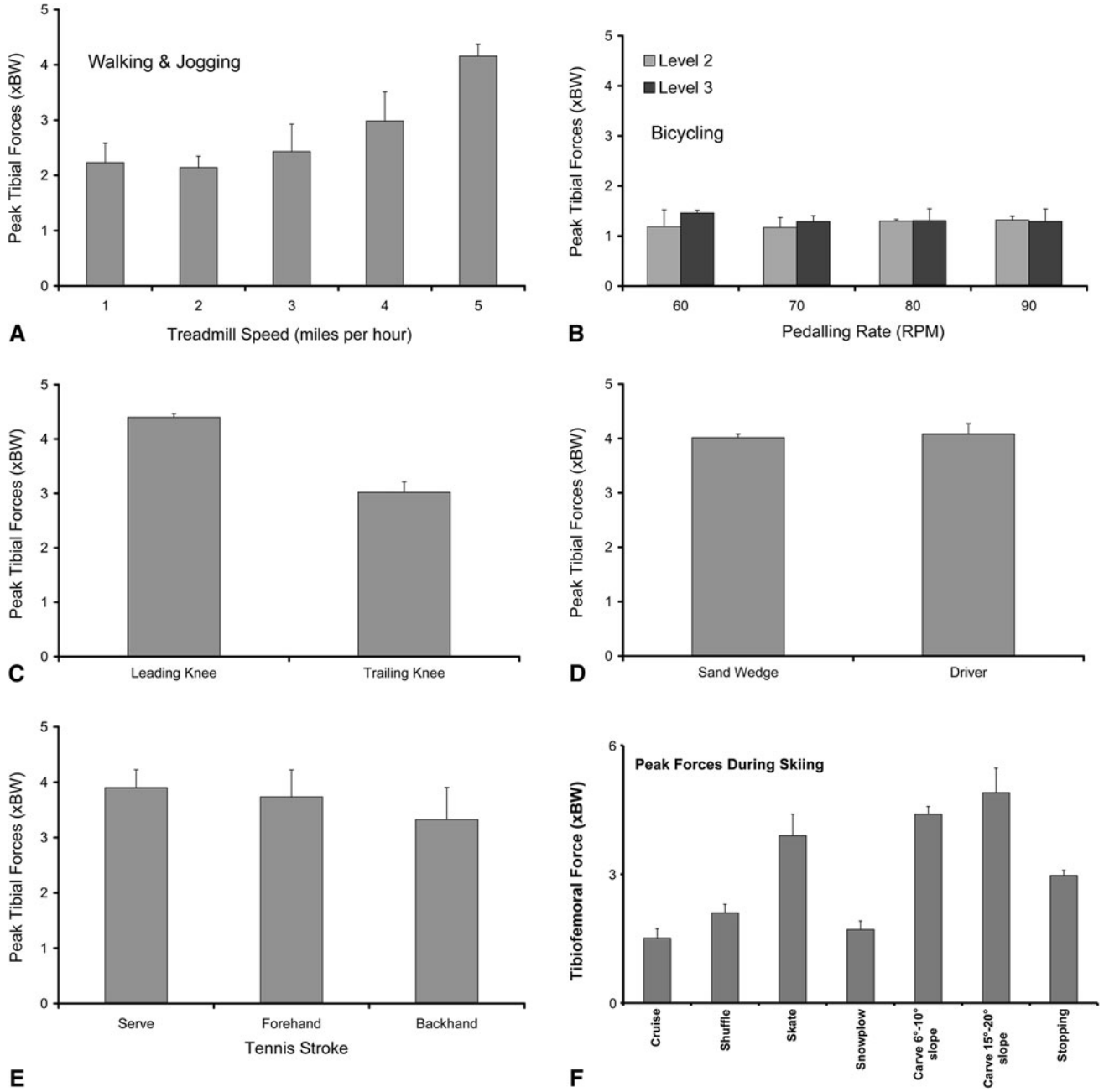

Fig. 5A–J The graphs show peak forces (± SD) generated during various recreational activities including (**A**) walking and jogging, (**B**) stationary biking, (**C**) with golf using a (**D**) sand wedge or driver, (**E**) tennis, (**F**) skiing, (**G**) elliptical trainer, (**H**) StairMaster®, (**I**), leg press, and (**J**) knee extensions exercises. (Published with permission from Springer Publishing Company from D'Lima DD, Steklov N, Patil S, Colwell CW Jr. The Mark Coventry Award: in vivo knee forces during recreation and exercise after knee arthroplasty. *Clin Orthop Relat Res.* 2008;466:2605–2611.)

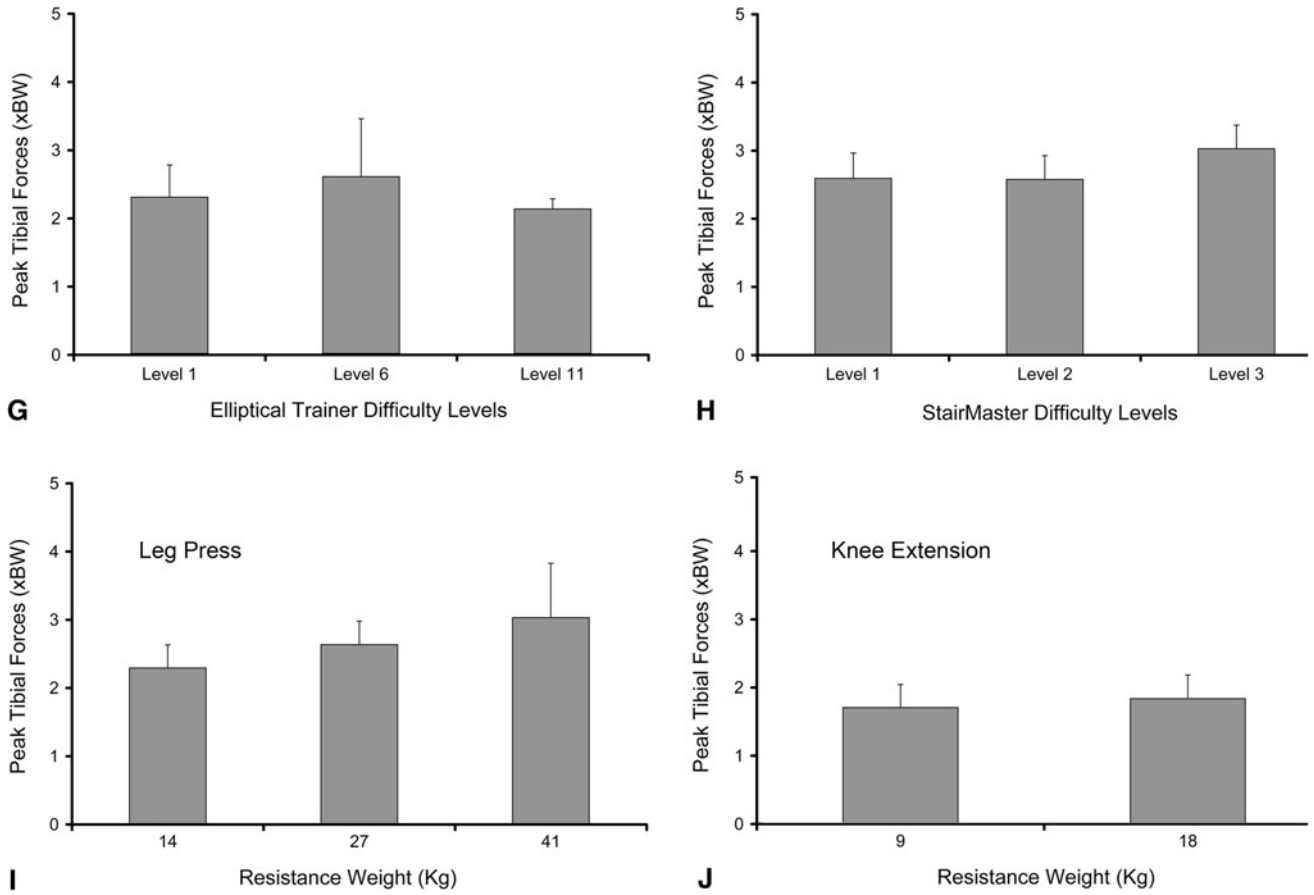

Fig. 5A–J continued

of $0.85 \pm 0.08 \times$ BW at a maximum flexion angle $90° \pm 1°$ (Fig. 5G, H). Exercising on the elliptical trainer (9500 HR; Life Fitness, Schiller Park, IL, USA) generated a mean peak tibial force of $2.24 \pm 0.22 \times$ BW, which remained unchanged with increasing levels of difficulty [14]. Anterior tibial shear forces were very low ($0.15 \pm 0.06 \times$ BW). Exercising on a stair-climbing machine (StairMaster® 4000 PT; Nautilus Inc, Vancouver, WA, USA) generated similar forces at lower levels of intensity but increased to greater than $3 \times$ BW at higher levels (Fig. 5H). The knee flexion angle at peak tibial forces increased with increasing intensity.

Leg-Press and Knee-Extension Machine

Tibial forces increased with increasing resistance during the leg press activity (Fig. 5I) but did not change during the knee extension activity (Fig. 5J). Leg-press and knee-extension activities generated similar magnitudes of peak AP shear ($0.24–0.35 \times$ BW) [14]. Shear was directed anteriorly during the leg-press activity and directed posteriorly in the knee-extension activity.

Stationary bicycling generated low tibial forces, whereas jogging and tennis generated high peak forces. The golf swing generated unexpectedly high forces especially in the leading knee. Exercise on the elliptical trainer generated lower forces than jogging but not lower than treadmill walking. Rowing machines often are recommended to increase knee flexion during rehabilitation; however, surgeons are cautious about recommending rowing after TKA [20]. Rowing generated the lowest peak knee forces of all recreational activities. The leg-press machine exercises similar muscles as the squat. One advantage of the leg-press machine is that resistance can be reduced to below body weight. The knee-extension exercise against resistance is a safe method of strengthening the quadriceps muscle without generating high tibial forces. The leg-press machine therefore can be recommended to build up to a squat if a full weightbearing squat is not possible.

These results support a scientific approach to recommending activities after TKA. Tibial forces comprise only one of the factors that may contribute to the potential for prosthetic wear and damage. Other factors include the kinematics, which affect contact area, and the number of

cycles of the activity. For example, the golf swing generated forces similar in magnitude to jogging. However, the number of cycles during which the knee is exposed to high forces during a golf game are fewer than the number of cycles during jogging. Continuous activity monitoring (third-generation device) using a wearable data acquisition system is ongoing. Activity-specific knee designs can now be designed, such as a knee design more tolerant of golfing, by optimizing the conflicting needs of increased rotational laxity and conformity.

Orthotics

Several studies have reported the knee adduction moment during walking is associated with the presence [2, 42] and rate of progression [36] of medial compartment knee osteoarthritis (OA) and has been used to predict the outcome of treatment interventions for OA [45]. Clinical and analytic studies [1, 46] associate external adduction moment with excessive loading of the medial compartment. The relationship between the knee adduction moment and medial compartment load has not been directly tested in vivo. We used orthotics to modulate the external adduction moment for comparison with medial compartmental tibial forces.

Tibial forces were measured while the subjects were wearing their own personal walking shoes and while wearing variable-stiffness shoes designed to reduce the adduction moment [16]. The variable-stiffness shoes had a sole with reduced stiffness on the medial side. The variable-stiffness intervention shoes reduced peak external knee adduction moment between 13% and 22%. Medial contact force also was significantly reduced by 10% to 19%.

The direct tibial force measurements confirmed the use of peak external adduction moment as a simple surrogate for medial compartment load. These results support clinical studies associating knee adduction moment with degradation of cartilage in the medial compartment of the knee. The shoes used in this study were effective in decreasing external knee adduction moment and medial compartmental loading. These results support the use of treatment modalities designed to reduce knee adduction moment to address medial compartment knee OA.

In Vivo Contact Stresses

Stresses at the bearing surface are a major factor in polyethylene wear and fatigue and affect the life of the implant. To date, polyethylene contact stresses have been calculated using computational models and have been measured in vitro with pressure sensors. Tibial forces used to generate contact stresses in previous studies have been mathematical estimates. We used tibial forces and knee kinematics measured in vivo to calculate contact stresses for activities of daily living [13].

Experimental Data

Tibial forces were recorded for level walking, stair climbing, and deep knee bend (kneel and lunge) activities. Knee kinematics were measured simultaneously using a validated fluoroscopic analysis technique [3]. A finite element model of the implanted knee was generated using MSC.MARC (MSC Software, Santa Ana, CA, USA).

Model Specifications

The femoral component and tibial tray were modeled as rigid bodies. The polyethylene insert was modeled using an elastoplastic material model [29]. For input into the finite element model, one set of kinematic and tibial force data was constructed from the synchronized experimental data for each activity.

Peak contact and von Mises stresses were computed for one entire cycle of level walking and stair climbing, and at maximum flexion angle during high-flexion activities. For comparison of contact stresses calculated in vivo with those generated during knee wear testing, we applied loading and boundary conditions using the International Standards Organization (ISO)-recommended conditions for knee wear simulation [21].

Walking

For comparison among conditions, the following three events during the gait cycle were chosen: peak tibial load after heel-strike (first peak), peak load before toe-off (second peak), and the lowest load during midstance. Peak contact stresses, mean contact stresses, and contact areas for gait at two speeds were similar [13]. The ISO loading waveform applies greater axial load (peak 2600 N) and therefore generated higher contact stresses. The peak contact stresses generated during the ISO simulation were associated with the peak before toe-off (30 MPa) and were approximately 18% higher than peak in vivo contact stresses calculated for the fast-gait activity. Walking is generally considered to be an activity that subjects the prosthetic components to benign stresses in a well-aligned knee. Our data support this consensus as peak stresses were less than those reported for yield strength of polyethylene.

Stair Climbing

Stair climbing generated higher total contact forces (peak 3.5 × BW) with concomitantly higher contact stresses [13]. The center of pressure moved posteriorly with knee flexion indicative of femoral rollback. Peak axial forces during the step-up activity were nearly 60% greater than during gait. Peak contact stresses increased by a more modest percentage (18%). This result was most likely attributable to the inclusion of plasticity in the material model. This resulted in a higher plastic strain during stair climbing, which contributed to the 29% increase in contact area during stair climbing relative to gait.

Deep-Flexion Activities

The subjects had an excellent range of knee flexion (> 130°). During kneeling, most of the external ground reaction force was transmitted through the anterior surface of the upper tibia. During the lunge activity, the ground reaction force was transmitted through the foot. The lunge activity generated modest knee contact forces (1.6 × BW) relative to walking and stair climbing [13] owing to the reduced contact area in deep flexion (less than 50% of the contact area calculated for stair climbing). Kneeling generated the lowest contact forces (0.3 × BW) and the lowest contact area (29 mm^2) owing to the poor femorotibial contact in deep flexion. Despite the low knee forces, kneeling resulted in peak contact stresses that were greater than those calculated for walking or stair climbing.

Restricted knee flexion is a significant complication preventing high flexion activities such as kneeling and gardening for Western populations, and squatting, kneeling, and sitting cross-legged for Eastern and Middle-Eastern populations. A common design feature of so called "high flexion" designs is to modify the articular geometry to increase the contact area between the tibial and femoral articular surfaces' high flexion angles. Our finding of high contact stresses during the lunge and kneeling activities (Fig. 6) owing to the small area of contact indicate that designs with a broader articular contact area at high flexion might reduce the risk for polyethylene damage [13].

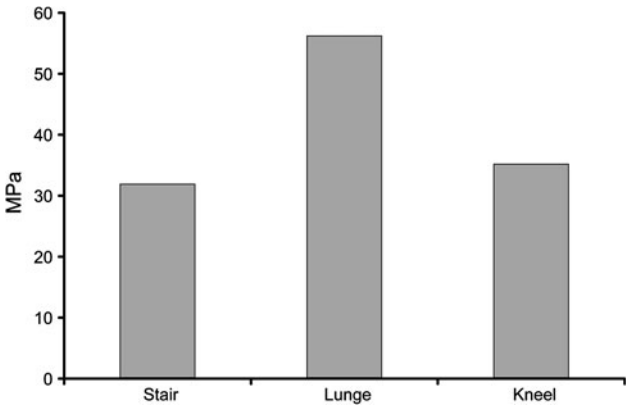

Fig. 6 Stair climbing generated higher contact stresses than walking. Both high flexion activities (lunge and kneel) generated even higher contact stresses, with the lunge activity generating the highest contact stresses. (Published with permission from John Wiley & Sons from D'Lima DD, Steklov N, Fregly BJ, Banks S, Colwell CW Jr. In vivo contact stresses during activities of daily living after knee arthroplasty. *J Orthop Res.* 2008;26:1549–1555.)

Evaluation of Predicted Knee Forces

The knee is a complex joint that is difficult to model accurately. Although advances have been made in mathematical models of the knee, the assumptions inherent in these models have yet to be substantiated. For the first time, in vivo measurement of tibial forces is available for evaluating computer models. Clinically applicable models can be used for evaluating the effects of design changes, different surgical techniques, and component alignment. Toward this goal, we developed dynamic computer models predicting knee forces that were evaluated using in vivo forces.

Subject-specific Parameters

Preoperative MR images (obtained before the implantation) were segmented and used to identify bony attachments of ligaments and tendons at the knee. Preoperative and postoperative CT scans were obtained and segmented to identify bony surface geometry and implant position and orientation. Limb measurements were used to calculate segment inertial properties.

Model Specifications

Computer-aided design (CAD) models of the femoral, tibial, and patellar components were obtained from the manufacturer (Zimmer Inc, Warsaw, IN, USA) and virtually "implanted" in the bony geometry obtained from the CT scans as previously described (Fig. 7) [25]. The soft tissues (collateral ligaments, posterior cruciate ligaments, patellar tendon, and quadriceps tendon) were modeled as nonlinear springs based on published data [31]. Contact between the quadriceps tendon and the trochlear groove in deep flexion was simulated using ellipsoids connected in series by nonlinear springs. The MSC.ADAMS dynamics engine was used to compute tibiofemoral and patellofemoral kinematics and contact forces.

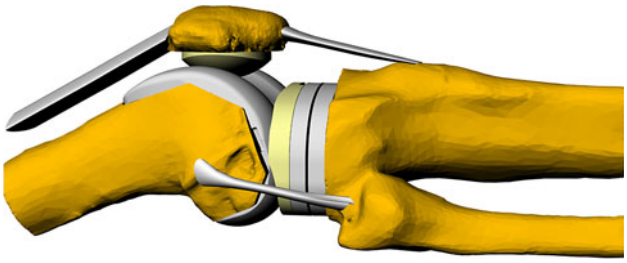

Fig. 7 A rigid body dynamic model of knee arthroplasty was constructed in MSC.ADAMS (MSC Software, Santa Ana, CA, USA).

Evaluation of Predicted Forces

Knee kinematics and forces were measured during dynamic knee extension with the subjects seated in a chair. Knee kinematics (tibial axial rotation, tibial adduction, femoral rollback) and tibial force were compared with those predicted by the model (Fig. 8). These results show the feasibility of predicting knee kinematics and forces using subject-specific parameters. Ongoing development of models includes activities of daily living, recreation, and exercise.

Calculating Knee Kinematics from Knee Forces

In addition to knee forces, knee kinematics are essential for a complete understanding of the biomechanics of the knee. Commonly used methods of measuring knee kinematics include video motion analysis of markers placed on the skin and dynamic fluoroscopy of the knee. The skin marker technique is most widely used but is prone to error because of the motion of the skin relative to the underlying bones. Dynamic fluoroscopy is much more accurate as the bones and implants are directly observed. The activities that can be analyzed are restricted by the risk of radiation exposure and the small field of view of the fluoroscope (approximately 1 foot square). Our objective was to develop a novel method of computing knee kinematics from forces measured using the electronic prosthesis.

In Vitro

We first tested proof of the concept that a unique relationship exists between relative implant position and contact force vector. An electronic tibial tray, along with a polyethylene insert and femoral component of matching size, was mounted on a multiaxial servohydraulic testing machine (Force5^{TM}; AMTI, Watertown, MA, USA). Tibial forces changed substantially with AP component alignment (Fig. 9). Medial shear and varus moment were similarly sensitive to translation in the mediolateral direction. Tibial forces were less sensitive to changes in flexion.

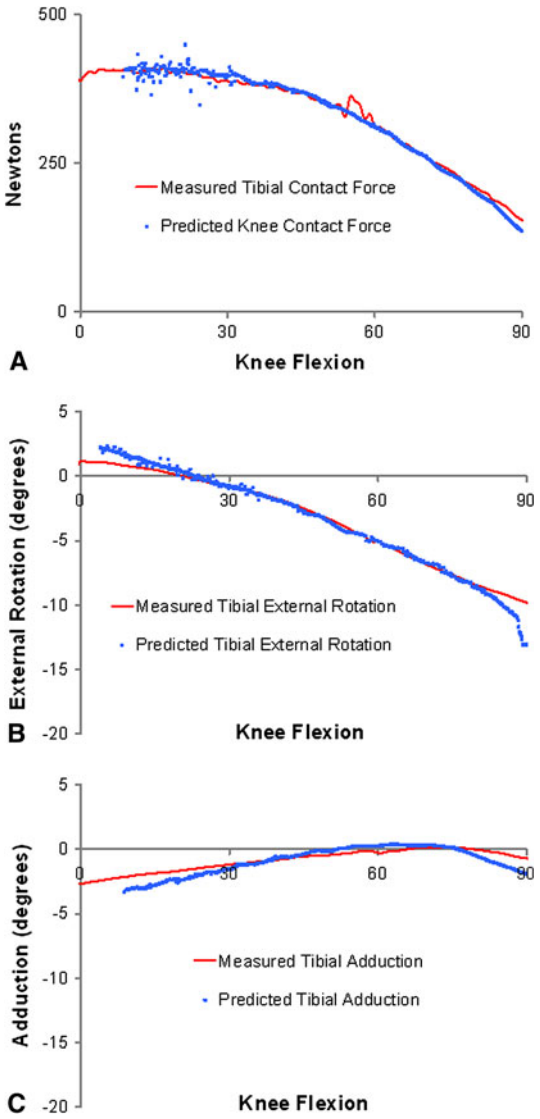

Fig. 8A–C The graphs show evaluation of the dynamic contact model with in vivo measured (**A**) tibial forces and knee kinematics [(**B**) external rotation and (**C**) adduction] during an open-kinetic chain knee extension activity. Close agreement between measured and predicted outcomes reflect the viability of a subject-specific modeling approach.

Computer Algorithm to Predict Knee Kinematics

An inverse finite element approach was used to determine if the tibial tray forces and moments could be used to compute the original tibiofemoral position used to generate the force data. A previously described finite element model was used to generate a training dataset of synthetic tibial tray forces and moments for a matrix of combinations of tibiofemoral orientations and positions [13]. The boundary conditions were varied as follows. Axial load was varied between 100 N and 2500 N; flexion was varied between −5° and 130°; adduction was varied between −3° and 3°;

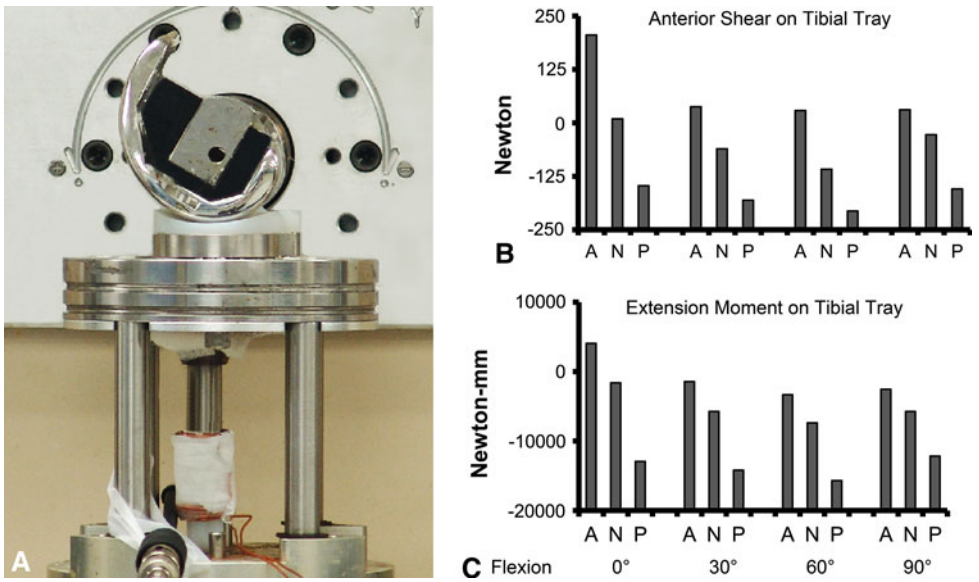

Fig. 9A–C (**A**) A tibial tray instrumented with a six-component load cell with a polyethylene insert and femoral component of matching size were mounted on the Force5^{TM} multiaxial servohydraulic testing machine. Tibial tray forces were recorded under vertical loads of 890 N (yellow arrow). Forces were recorded under AP and mediolateral translation of the femoral component relative to the insert, and s axial rotation, varus-valgus angulation, and flexion. Tibial forces [(**B**) anterior shear and (**C**) extension moment] changed substantially with AP component alignment. Tibial forces were less sensitive to changes in flexion. A = 5 mm anterior; N = neutral position; P = 5 mm posterior.

axial rotation was varied between −15° and 15°; anterior translation was varied between −15 mm and 10 mm; and lateral translation was varied between −3 mm and 3 mm. An optimization algorithm was developed in a commercially available program (iSIGHT, Simulia, Providence, RI, USA) that incorporated the finite element model to compute knee kinematics from knee forces (Fig. 10). The femur was flexed using the knee flexion angle from the training dataset and brought into contact with the fixed tibial insert using the three-component contact force vector from the dataset applied as boundary conditions to the femoral component. The femur was free to translate in all directions. Femorotibial adduction-abduction and axial rotation were optimized to minimize the difference between the resultant moments output by the model and the experimentally measured moments. The objective of this approach was to compute the relative tibiofemoral position for a given flexion angle and six-component force and moment vector. The algorithm was refined until the target average absolute errors in predicting synthetic position data were less than 0.5 mm in AP and mediolateral translation and less than 0.5° in axial rotation and adduction-abduction.

In Vivo

Previously reported knee forces and fluoroscopic kinematics measured during walking, stair ascent, dynamic single-leg lunge, and chair rising-sitting were used to evaluate the inverse finite element optimization algorithm [13, 55, 61]. From each implanted subject, 10 different force and kinematic vectors were selected. A finite element model was constructed for each subject as previously described [13]. In vitro pilot testing and optimization on synthetic data indicated that the accuracy of the algorithm was unacceptable for knee flexion angle. Therefore knee flexion was not predicted but was included as an input in addition to the knee forces and moments. The femur was flexed using the fluoroscopically measured knee flexion angle and brought into contact with the fixed tibial insert using the measured three-component contact force vector applied as boundary conditions to the femoral component. The femur was free to translate in all directions to satisfy the constraints of the force vector. Femorotibial adduction-abduction and axial rotation were optimized to minimize the difference between the resultant moments output by the model and the experimentally measured moments. Average absolute errors were less than 1.2 mm in AP and mediolateral translation, 1.6° for axial rotation, and 0.8° for varus-valgus angulation.

We developed a novel and accurate method of computing knee kinematics directly from in vivo measured knee forces and knee flexion angle. We used a custom electrogoniometer for subsequent experiments to measure knee flexion. The average absolute error in electrogoniometer-measured flexion when compared with fluoroscopic-measured flexion was 6°. This algorithm

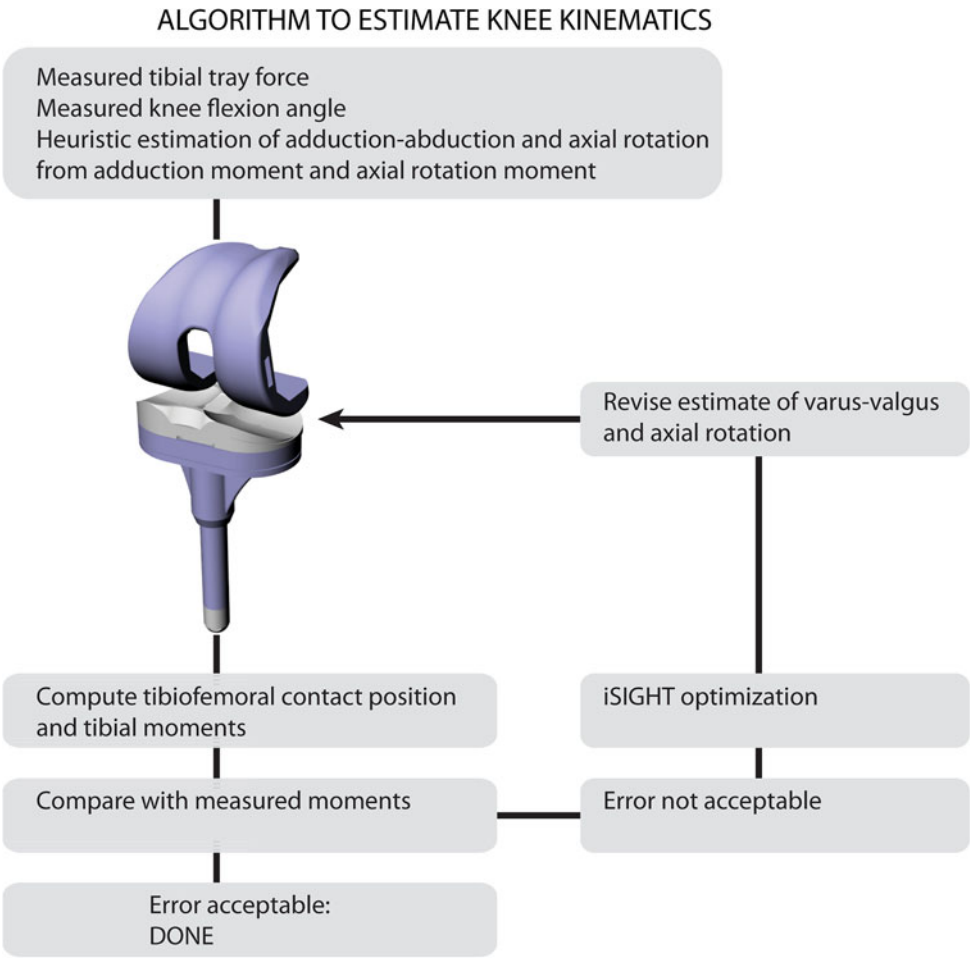

Fig. 10 A diagram illustrates the algorithm to determine knee kinematics from knee forces. A tibial tray instrumented with a six-component load cell with a polyethylene insert and a finite element model was used. The femur was flexed using the measured knee flexion angle and brought into contact with the tibial insert. The three-component contact force vector (axial force, medial shear, and anterior shear) was applied as boundary conditions to the femoral component, which was free to translate in all directions. The relative femorotibial adduction-abduction and axial rotation were varied using an optimization software (iSIGHT, Apple, Cupertino, CA, USA) until the difference between the resultant moments output by the model and the experimentally measured moments was less than 1%. The finite element analysis directly solves for the contact position based on the three-dimensional contact force vector as part of the prescribed boundary conditions, thus yielding the alignment in AP and mediolateral directions. Therefore, in the optimization step, only the three moments have to be matched to the experimental data.

greatly leverages the utility of the electronic knee prosthesis in capturing knee motion and forces without extensive external laboratory equipment. Because we use contact analysis to compute kinematics, we obtained a near-complete biomechanical assessment of each activity. This combination of implantable and wearable hardware with software analysis essentially creates a 'lab-in-a-knee'.

A Wearable Force and Kinematics Monitoring Device

The electronic prosthesis is powered wirelessly by a large circular inductor coil fitted around the patient's knee to power the small internal coil in the implanted prosthesis [12, 15]. A 2400-W audio amplifier, driven by a 6.9-KHz sine wave signal, was used to power the inductor coil. A radio frequency receiver and laptop computer captured the wireless data signal. The total weight of powering and data acquisition equipment including the amplifier, function generator, receiver, and laptop computer was more than 90 pounds. The patient was effectively tethered to the power supply by a 20-foot cable, restricting the patient's motion to a small volume (Fig. 11). We therefore developed a third-generation wearable powering and data acquisition system. We replaced the original "air core" inductor coil with a 2-inch–long ferrite core coil (Fig. 12), which produced a sufficiently powerful electromagnetic field. The audio amplifier, function generator, and inductor coil were redesigned to fit a wearable belt pack, weighing less than 2 pounds. The original inductor coil circuit was

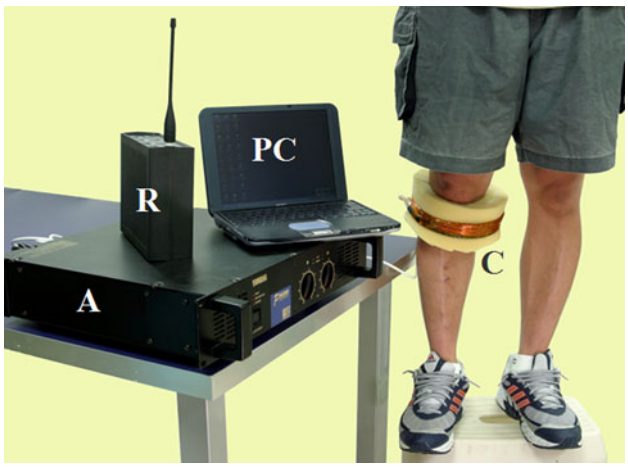

Fig. 11 The original data acquisition system is shown. The force transducers and telemetry system in the instrumented tibial prosthesis were powered wirelessly by coil induction. A large circular inductor coil (C) was fitted around the patient's knee to power the small internal coil within the implanted prosthesis. The inductor coil is 6 inches in diameter with 20 turns of Number 14 Teflon®-coated copper wire and a measured inductance of 0.97 mH. A 2400-W audio amplifier (A), driven by a 6.9-KHz sine wave signal (generated by a function generator), was used to power the inductor coil. During normal operation of the electronic prosthesis, 15 to 20 A of current flows between the inductor coil and the audio amplifier. A radio frequency receiver (R) and laptop computer (PC) capture the wireless data signal. The total weight of powering equipment for the instrumented prosthesis including the amplifier, function generator, receiver, and laptop computer was more than 90 pounds. The patient was tethered to the power supply by a 20-foot cable, restricting the patient's motion to a small volume.

replaced with a series inductor-capacitor resonant circuit. As knee flexion is required for computing the rest of the knee kinematic components, an electrogoniometer was incorporated in a knee sleeve that housed the power induction coil.

Almost all reported motion analyses of the knee involve activities under carefully controlled laboratory settings. These activities are artificially constrained primarily owing to the restrictions imposed by the data acquisition equipment.

Controlled activities are most likely substantially different from unsupervised activities. In two subjects, accidental stumbling generated some of the highest recorded in vivo hip loads (greater than 8 × BW) [4]. Few studies have attempted to monitor unsupervised knee kinematics [39], and none have continuously monitored knee contact forces. Our third-generation device records knee forces and knee kinematics simultaneously at a data acquisition rate of as much as 80 Hz, which compares favorably with traditional fluoroscopic analysis (30 Hz) or commercially available accelerometer-based activity monitors (32 Hz; IDEEA; MiniSun, Fresno, CA, USA). The process of data capture is greatly simplified and artificial constraints imposed by laboratory equipment are negligible.

Knee force and knee flexion data from 100 walking cycles (Fig. 13), 100 stair-climbing cycles, 200 chair-rise cycles, and 600 cycles of random data collected during

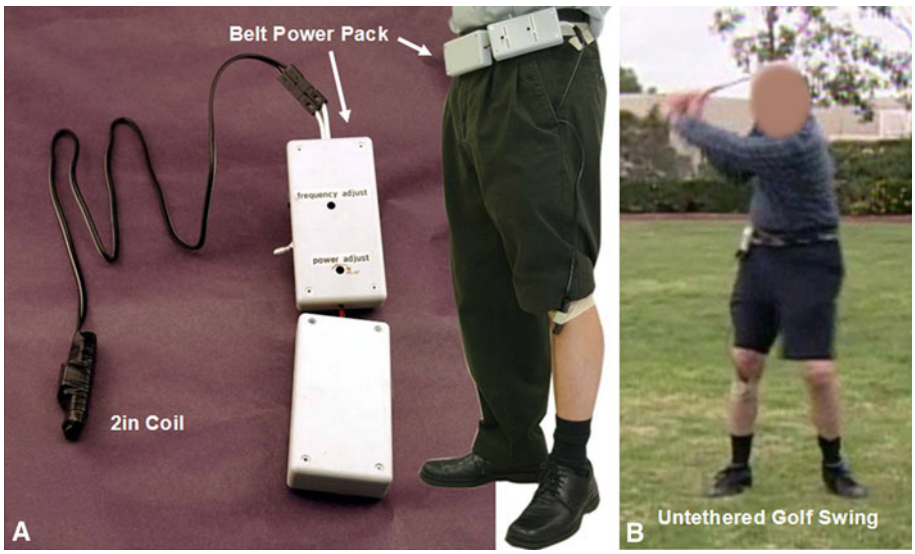

Fig. 12A–B (**A**) A photograph shows the miniaturization of the power equipment. The audio amplifier, function generator, and inductor coil were redesigned to fit a wearable belt pack form factor. The original inductor coil circuit was replaced with a series inductor-capacitor resonant circuit. A capacitor was implemented in series with the inductor coil and the circuit resonant frequency was tuned to the telemetry system (6.9 KHz). This reduced power requirements by 15-fold (to less than 1 A). The 2400-W amplifier was replaced with a switching NPN-PNP transistor driver. The transistors are switched on and off rapidly by a standard timer chip integrated circuit (IC 555) resulting in current flow back and forth between the inductor coil and the capacitor. A square wave pulse generator was built on the IC 555 and replaced the original sine wave function generator. The entire power supply for the instrumented prosthesis fits into a belt pack and weighs less than 2 pounds (including batteries). (**B**) A photograph shows a subject with a portable power pack.

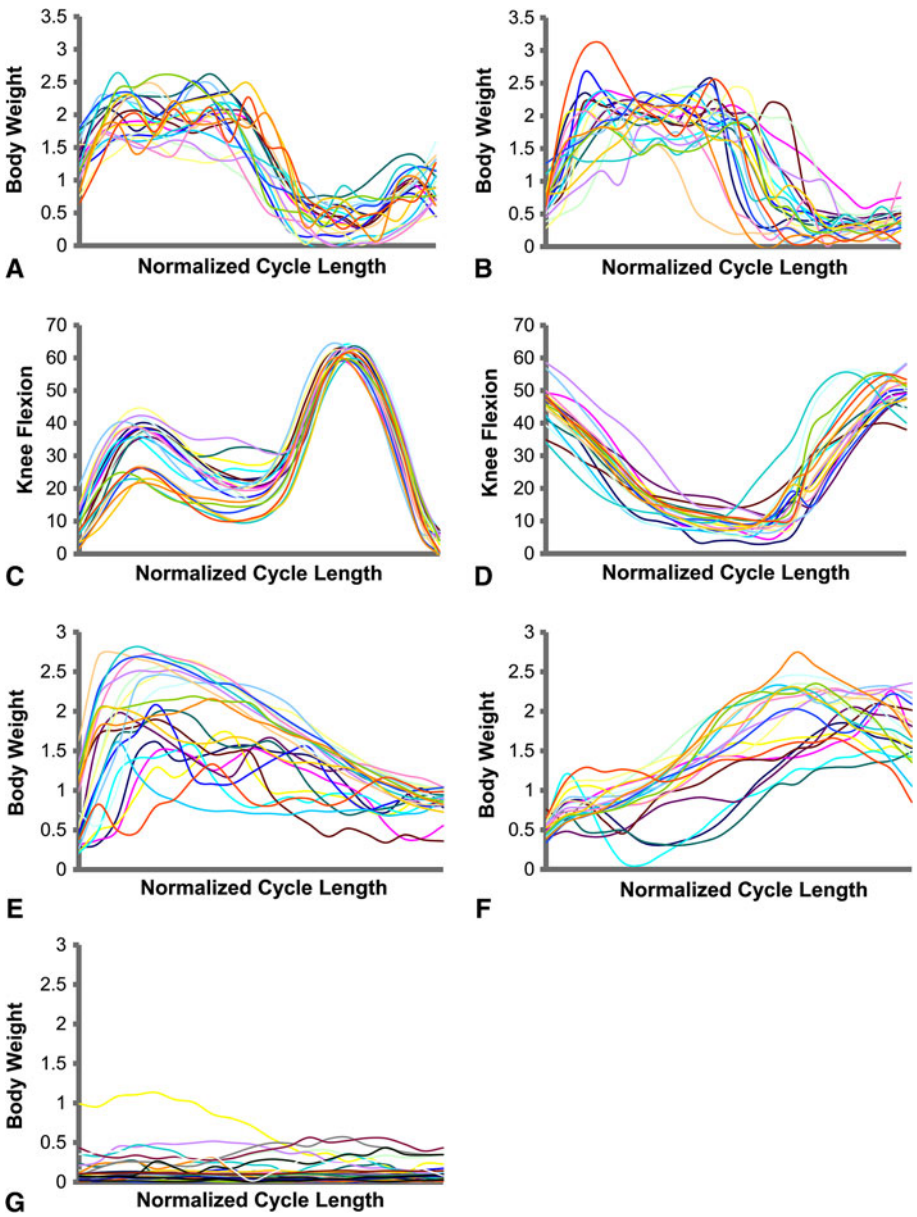

Fig. 13A–G The graphs show validation datasets used to test the activity classification algorithm: (**A**) axial load cycles for walking, (**B**) axial load cycles for stair climbing, (**C**) flexion cycles for walking, (**D**) flexion cycles for stair climbing, (**E**) axial load cycles for chair sit-to-stand, (**F**) axial load cycles for chair stand-to-sit, and (**G**) random cycles of inactivity.

periods of inactivity were compiled. The rationale for selecting these activities were clinical relevance, high frequency of occurrence, range of flexion covered (from 0° to ~ 100°), and the availability of sufficient data samples. The data were divided into 50% training, 25% testing, and 25% validating subsets. The training data subsets were used to train a multilayered feed-forward backpropagation neural network constructed using the Neural Network Toolbox in Matlab® R13 (The Mathworks, Natick, MA, USA). After training, the network was evaluated using data set aside for validation (the 25% data subset not used in training or testing). In Phase I, only the vertical axial contact force was used as an input to train a network. The network was 100% successful in separately classifying walking and chair-rise activities. This result was anticipated as the force curves were substantially different (Fig. 13). A previously reported classification system entirely based on knee flexion angle and the angles of the thigh and calf overestimated walking by approximately 11% and underestimated stair climbing by approximately 8% [39]. However, our accuracy of classifying force curves for walking and stair climbing decreased to between 50% and 62%. As the flexion curves for walking and stair climbing were substantially different, we retrained the network with axial force and flexion angle input vectors. Including the knee flexion angle dramatically increased accuracy to 100%. In Phase II, our objective was to separate the chair-rise activity into sit-to-stand and stand-to-sit portions. The axial force tends to peak earlier in the sit-to-stand than in the stand-to-sit activity (Fig. 13E, F).

With axial load and flexion angle as inputs, the network was able to correctly classify 100% of the trials. A similar strategy was used to differentiate stair ascent from descent.

Work is ongoing to clarify and classify unsupervised activities and to determine the accuracy of classifying other activities. The wearable hardware is currently being field tested for up to 7 days of continuous monitoring.

Discussion

Knee forces and kinematics traditionally have been measured under laboratory conditions. Although this approach is useful for quantitative measurements and experimental studies, the extrapolation of results to clinical conditions may not always be valid. In the laboratory, subjects are instructed to perform carefully choreographed activities under artificial conditions to satisfy constraints of the testing equipment. We therefore developed a third generation of wearable monitoring equipment to permit measurements outside the laboratory. As knee kinematics are an important component of biomechanical analysis, we developed a novel method of computing knee kinematics using the measured in vivo force. Finally, we used a neural network-based pattern classification algorithm for classifying and identifying unsupervised activities.

There are some limitations related to our studies. First is the small sample size, which does not permit extrapolation of our results to a larger patient population or other implant designs. Second, we could not accurately compute knee flexion and therefore it required measurement. We therefore combined an electrogoniometer in the wearable data acquisition apparatus. Third, the electronic prosthesis is not commercially available. Owing to the high cost and the fact that it does not directly improve clinical outcomes, it remains a research tool. We are working on developing lower-cost implantable sensors, which also provide real-time feedback to the patient with the ability to identify activities at high risk for implant damage or failure.

The pattern classification is a learning algorithm. As we continue to add to our database of knee forces measured under a wide spectrum of conditions, the pattern classification algorithm becomes more robust. Although we have been successful in classifying previously collected data from several different clinically relevant activities of daily living, it is not likely that all unsupervised activities will be quite as easily identified. The present version of the electrogoniometer uses a rotational potentiometer to measure knee flexion. We now are using angular wireless sensors with embedded accelerometers, gyroscopes, and magnetometers to determine knee angles and thigh and lower leg angular position relative to gravity, which will provide valuable information for classifying activities. Combining our technology with other wearable activity monitoring systems that monitor whole body kinematics also will be useful in identifying and classifying kinematics of the entire body during unsupervised activities.

Contact analysis often is used to identify activities at high risk to the implant and implant-bone interface [13, 52]. As we use finite element-based contact analysis to compute knee kinematics from knee forces, in addition to knee forces and knee kinematics we also obtain contact area, contact stresses, and the distribution of local stresses and strains. Combining this analysis with custom models of the bone (eg, using CT scans) can be a powerful tool for providing more complete and subject-specific predictions of implant wear, damage, and risk of failure [60].

This method of obtaining combined kinematics and forces with minimal external hardware greatly increases our ability for capturing true kinematics and forces. Activities outside the laboratory generated significantly different forces compared with in-laboratory measurements. Clinically relevant data can be obtained for preclinical testing of prostheses and for advising patients regarding postoperative rehabilitation and activities. Continuously monitoring in vivo knee forces and kinematics under real-life conditions can identify weaknesses and potential areas of failure in current designs and provide direction to enhancing the function and durability of TKA.

Acknowledgments These studies have been possible because of active collaborations with Benjamin J. Fregly, PhD, University of Florida; Thomas Andriacchi PhD, Stanford University; Scott Banks PhD, BioMotion Foundation; Harry Rubash MD, and Guoan Li PhD, Harvard Medical Center; Ritchie Gill PhD, Oxford, UK; Richard Komistek PhD, University of Tennessee; Marcus Pandy PhD, Sydney, Australia; and Urs Wyss PhD, Calgary, Canada. In addition, the following allowed us to use their facilities: the TaylorMade Performance Lab, Carlsbad, CA; the Torrey Pines Golf Course, La Jolla, CA; and the La Jolla Beach and Tennis Club, La Jolla, CA.

References

1. Andriacchi TP. Dynamics of knee malalignment. *Orthop Clin North Am.* 1994;25:395–403.
2. Baliunas AJ, Hurwitz DE, Ryals AB, Karrar A, Case JP, Block JA, Andriacchi TP. Increased knee joint loads during walking are present in subjects with knee osteoarthritis. *Osteoarthritis Cartilage.* 2002;10:573–579.
3. Banks SA, Hodge WA. Accurate measurement of three-dimensional knee replacement kinematics using single-plane fluoroscopy. *IEEE Trans Biomed Eng.* 1996;43:638–649.
4. Bergmann G, Graichen F, Rohlmann A. Hip joint loading during walking and running, measured in two patients. *J Biomech.* 1993;26:969–990.
5. Brand RA, Pedersen DR, Davy DT, Kotzar GM, Heiple KG, Goldberg VM. Comparison of hip force calculations and measurements in the same patient. *J Arthroplasty.* 1994;9:45–51.
6. Collins JJ. The redundant nature of locomotor optimization laws. *J Biomech.* 1995;28:251–267.

7. Denis K, Van Ham G, Bellemans J, Labey L, Sloten JV, Van Audekercke R, Van der Perre G, De Schutter J. How correctly does an intramedullary rod represent the longitudinal tibial axes? *Clin Orthop Relat Res.* 2002;397:424–433.
8. Diduch DR, Insall JN, Scott WN, Scuderi GR, Font-Rodriguez D. Total knee replacement in young, active patients: long-term follow-up and functional outcome. *J Bone Joint Surg Am.* 1997; 79:575–582.
9. D'Lima DD, Patil S, Steklov N, Chien S, Colwell CW Jr. In vivo knee moments and shear after total knee arthroplasty. *J Biomech.* 2007;40(suppl 1):S11–S17.
10. D'Lima DD, Patil S, Steklov N, Colwell CW Jr. An ABJS Best Paper: Dynamic intraoperative ligament balancing for total knee arthroplasty. *Clin Orthop Relat Res.* 2007;463:208–212.
11. D'Lima DD, Patil S, Steklov N, Slamin JE, Colwell CW Jr. The Chitranjan Ranawat Award: in vivo knee forces after total knee arthroplasty. *Clin Orthop Relat Res.* 2005;440:45–49.
12. D'Lima DD, Patil S, Steklov N, Slamin JE, Colwell CW Jr. Tibial forces measured in vivo after total knee arthroplasty. *J Arthroplasty.* 2006;21:255–262.
13. D'Lima DD, Steklov N, Fregly BJ, Banks S, Colwell CW Jr. In vivo contact stresses during activities of daily living after knee arthroplasty. *J Orthop Res.* 2008;26:1549–1555.
14. D'Lima DD, Steklov N, Patil S, Colwell CW Jr. The Mark Coventry Award: in vivo knee forces during recreation and exercise after knee arthroplasty. *Clin Orthop Relat Res.* 2008; 466:2605–2611.
15. D'Lima DD, Townsend CP, Arms SW, Morris BA, Colwell CW Jr. An implantable telemetry device to measure intra-articular tibial forces. *J Biomech.* 2005;38:299–304.
16. Erhart JC, Dyrby CO, D'Lima DD, Colwell CW, Andriacchi TP. Changes in in vivo knee loading with a variable-stiffness intervention shoe correlate with changes in the knee adduction moment. *J Orthop Res.* 2010;28:1548–1553.
17. Fregly BJ, Banks SA, D'Lima DD, Colwell CW Jr. Sensitivity of knee replacement contact calculations to kinematic measurement errors. *J Orthop Res.* 2008;26:1173–1179.
18. Fregly BJ, D'Lima DD, Colwell CW Jr. Effective gait patterns for offloading the medial compartment of the knee. *J Orthop Res.* 2009;27:1016–1021.
19. Hart R, Janecek M, Chaker A, Bucek P. Total knee arthroplasty implanted with and without kinematic navigation. *Int Orthop.* 2003;27:366–369.
20. Healy WL, Iorio R, Lemos MJ. Athletic activity after joint replacement. *Am J Sports Med.* 2001;29:377–388.
21. International Standards Organization. Standard number 14243-3: Implants for surgery; Wear of total knee joint prostheses: Part 3: Loading and displacement parameters for wear-testing machines with displacement control and corresponding environmental conditions for test. Geneva, Switzerland. 2000.
22. Jones DL, Cauley JA, Kriska AM, Wisniewski SR, Irrgang JJ, Heck DA, Kwoh CK, Crossett LS. Physical activity and risk of revision total knee arthroplasty in individuals with knee osteoarthritis: a matched case-control study. *J Rheumatol.* 2004;31: 1384–1390.
23. Kaufman KR, An KN, Litchy WJ, Morrey BF, Chao EY. Dynamic joint forces during knee isokinetic exercise. *Am J Sports Med.* 1991;19:305–316.
24. Kaufman KR, Kovacevic N, Irby SE, Colwell CW. Instrumented implant for measuring tibiofemoral forces. *J Biomech.* 1996;29: 667–671.
25. Kessler O, Patil S, Colwell CW Jr, D'Lima DD. The effect of femoral component malrotation on patellar biomechanics. *J Biomech.* 2008;41:3332–3339.
26. Kirking B, Krevolin J, Townsend C, Colwell CW Jr, D'Lima DD. A multiaxial force-sensing implantable tibial prosthesis. *J Biomech.* 2006;39:1744–1751.
27. Komistek RD, Kane TR, Mahfouz M, Ochoa JA, Dennis DA. Knee mechanics: a review of past and present techniques to determine in vivo loads. *J Biomech.* 2005;38:215–228.
28. Komistek RD, Stiehl JB, Dennis DA, Paxson RD, Soutas-Little RW. Mathematical model of the lower extremity joint reaction forces using Kane's method of dynamics. *J Biomech.* 1998;31: 185–189.
29. Kurtz SM, Pruitt L, Jewett CW, Crawford RP, Crane DJ, Edidin AA. The yielding, plastic flow, and fracture behavior of ultra-high molecular weight polyethylene used in total joint replacements. *Biomaterials.* 1998;19:1989–2003.
30. Lavernia CJ, Sierra RJ, Hungerford DS, Krackow K. Activity level and wear in total knee arthroplasty: a study of autopsy retrieved specimens. *J Arthroplasty.* 2001;16:446–453.
31. Li G, Gil J, Kanamori A, Woo SL. A validated three-dimensional computational model of a human knee joint. *J Biomech Eng.* 1999;121:657–662.
32. Lotke PA, Ecker ML. Influence of positioning of prosthesis in total knee replacement. *J Bone Joint Surg Am.* 1977;59:77–79.
33. Lutz GE, Palmitier RA, An KN, Chao EY. Comparison of tibiofemoral joint forces during open-kinetic-chain and closed-kinetic-chain exercises. *J Bone Joint Surg Am.* 1993;75:732–739.
34. Maxwell SM, Hull ML. Measurement of strength and loading variables on the knee during Alpine skiing. *J Biomech.* 1989; 22:609–624.
35. Mintz L, Tsao AK, McCrae CR, Stulberg SD, Wright T. The arthroscopic evaluation and characteristics of severe polyethylene wear in total knee arthroplasty. *Clin Orthop Relat Res.* 1991;273: 215–222.
36. Miyazaki T, Wada M, Kawahara H, Sato M, Baba H, Shimada S. Dynamic load at baseline can predict radiographic disease progression in medial compartment knee osteoarthritis. *Ann Rheum Dis.* 2002;61:617–622.
37. Mont MA, Marker DR, Seyler TM, Gordon N, Hungerford DS, Jones LC. Knee arthroplasties have similar results in high- and low-activity patients. *Clin Orthop Relat Res.* 2007;460:165–173.
38. Mont MA, Rajadhyaksha AD, Marxen JL, Silberstein CE, Hungerford DS. Tennis after total knee arthroplasty. *Am J Sports Med.* 2002;30:163–166.
39. Morlock M, Schneider E, Bluhm A, Vollmer M, Bergmann G, Muller V, Honl M. Duration and frequency of every day activities in total hip patients. *J Biomech.* 2001;34:873–881.
40. Morris BA, D'Lima DD, Slamin J, Kovacevic N, Arms SW, Townsend CP, Colwell CW Jr. e-Knee: evolution of the electronic knee prosthesis. Telemetry technology development. *J Bone Joint Surg Am.* 2001;83(suppl 2):62–66.
41. Morrison JB. The mechanics of the knee joint in relation to normal walking. *J Biomech.* 1970;3:51–61.
42. Mundermann A, Dyrby CO, Hurwitz DE, Sharma L, Andriacchi TP. Potential strategies to reduce medial compartment loading in patients with knee osteoarthritis of varying severity: reduced walking speed. *Arthritis Rheum.* 2004;50:1172–1178.
43. Nisell R, Ericson MO, Nemeth G, Ekholm J. Tibiofemoral joint forces during isokinetic knee extension. *Am J Sports Med.* 1989;17:49–54.
44. Patil S, Steklov N, Chien S, Colwell CW Jr, D'Lima DD. An analysis of in vivo knee forces while rising from a chair after knee arthroplasty. *Transactions of the 53rd Annual Meeting of the Orthopaedic Research Society*. San Diego, CA. 2007: Poster No 1836.
45. Prodromos CC, Andriacchi TP, Galante JO. A relationship between gait and clinical changes following high tibial osteotomy. *J Bone Joint Surg Am.* 1985;67:1188–1194.

46. Schipplein OD, Andriacchi TP. Interaction between active and passive knee stabilizers during level walking. *J Orthop Res.* 1991;9:113–119.
47. Seireg A, Arvikar. The prediction of muscular load sharing and joint forces in the lower extremities during walking. *J Biomech.* 1975;8:89–102.
48. Sharkey PF, Hozack WJ, Rothman RH, Shastri S, Jacoby SM. Insall Award paper. Why are total knee arthroplasties failing today? *Clin Orthop Relat Res.* 2002;404:7–13.
49. Simpson DJ, Gray H, D'Lima D, Murray DW, Gill HS. The effect of bearing congruency, thickness and alignment on the stresses in unicompartmental knee replacements. *Clin Biomech (Bristol, Avon).* 2008;23:1148–1157.
50. Sparmann M, Wolke B, Czupalla H, Banzer D, Zink A. Positioning of total knee arthroplasty with and without navigation support: a prospective, randomised study. *J Bone Joint Surg Br.* 2003;85:830–835.
51. Stockl B, Nogler M, Rosiek R, Fischer M, Krismer M, Kessler O. Navigation improves accuracy of rotational alignment in total knee arthroplasty. *Clin Orthop Relat Res.* 2004;426:180–186.
52. Szivek JA, Anderson PL, Benjamin JB. Average and peak contact stress distribution evaluation of total knee arthroplasties. *J Arthroplasty.* 1996;11:952–963.
53. Taylor WR, Heller MO, Bergmann G, Duda GN. Tibio-femoral loading during human gait and stair climbing. *J Orthop Res.* 2004;22:625–632.
54. Teter KE, Bregman D, Colwell CW Jr. Accuracy of intramedullary versus extramedullary tibial alignment cutting systems in total knee arthroplasty. *Clin Orthop Relat Res.* 1995;321:106–110.
55. Varadarajan KM, Moynihan AL, D'Lima D, Colwell CW, Li G. In vivo contact kinematics and contact forces of the knee after total knee arthroplasty during dynamic weight-bearing activities. *J Biomech.* 2008;41:2159–2168.
56. Walter JP, D'Lima DD, Colwell CW Jr, Fregly BJ. Decreased knee adduction moment does not guarantee decreased medial contact force during gait. *J Orthop Res.* 2010;28:1348–1354.
57. Weiner DK, Long R, Hughes MA, Chandler J, Studenski S. When older adults face the chair-rise challenge: a study of chair height availability and height-modified chair-rise performance in the elderly. *J Am Geriatr Soc.* 1993;41:6–10.
58. Wilk KE, Escamilla RF, Fleisig GS, Barrentine SW, Andrews JR, Boyd ML. A comparison of tibiofemoral joint forces and electromyographic activity during open and closed kinetic chain exercises. *Am J Sports Med.* 1996;24:518–527.
59. Windsor RE, Scuderi GR, Moran MC, Insall JN. Mechanisms of failure of the femoral and tibial components in total knee arthroplasty. *Clin Orthop Relat Res.* 1989;248:15–19; discussion 19–20.
60. Wong J, Steklov N, Patil S, Flores-Hernandez C, Kester M, Colwell CW Jr, D'Lima DD. Predicting the effect of tray malalignment on risk for bone damage and implant subsidence after total knee arthroplasty. *J Orthop Res.* 2011;29:347–353.
61. Zhao D, Banks SA, D'Lima DD, Colwell CW Jr, Fregly BJ. In vivo medial and lateral tibial loads during dynamic and high flexion activities. *J Orthop Res.* 2007;25:593–602.
62. Zhao D, Banks SA, Mitchell KH, D'Lima DD, Colwell CW Jr, Fregly BJ. Correlation between the knee adduction torque and medial contact force for a variety of gait patterns. *J Orthop Res.* 2007;25:789–797.